ORGANIC LETTERS

2010
Vol. 12, No. 11
2646−2649

Single-Electron Transfer Driven Cyanide Sensing: A New Multimodal Approach

M. R. Ajayakumar and Pritam Mukhopadhyay*

Supramolecular and Material Chemistry Lab, School of Physical Sciences, Jawaharlal Nehru University, New Delhi 110067, India

Sarita Yadav and Subhasis Ghosh

School of Physical Sciences, Jawaharlal Nehru University, New Delhi 110067, India

m_pritam@mail.jnu.ac.in

Received April 15, 2010

ABSTRACT

A new SET-driven reaction-based strategy is reported for sensing of cyanide with indicators having low LUMO levels. The cyanide-specific reaction produces an air-stable radical anion marker and by virtue of its spin, charge, and the SOMO-LUMO-based electronic transition generates multimodal signal outputs. High selectivity and sensitivity (0.2−16 μM) were observed when compared to other reducing anions. This new indicator system exhibits regenerability and dip-stick sensing, and fabrication of an electronic sensing device for cyanide is demonstrated.

There is continuous effort toward the design of anion sensors based on small molecules and their ensembles.[1] Among the anions, cyanide has evinced maximum interest due to its severe toxicity. Recently, reaction-based indicators/chemodosimeters have evolved as an attractive platform for sensing cyanide anions[2] and other analytes.[3] Cyanide sensors are also based on H-bonding, time-gated fluorescence, metal ion complexes, conformational changes, quantum dots, and thin-film sensing.[4a−h]

Cyanide sensing with reaction-based indicators utilizes the nucleophilic nature of the cyanide, and the design comprises a substrate and a reporter unit. Functional groups such as carbonyl/ene/imine[5] or Lewis acidic boranes[6] are used as substrates, while π-conjugated chromophores are used as the reporter units (Scheme 1a).

(1) (a) Beer, P. D.; Gale, P. A. *Angew. Chem., Int. Ed.* **2001**, *40*, 486–516. (b) Lavigne, J. J.; Anslyn, E. V. *Angew. Chem., Int. Ed.* **2001**, *40*, 3118–3130. (c) Martínez-Máñez, R.; Sancenón, F. *Chem. Rev.* **2003**, *103*, 4419–4476. (d) Sessler, J. L.; Seidel, D. *Angew. Chem., Int. Ed.* **2003**, *42*, 5134–5175. (e) Best, M. D.; Tobey, S. L.; Anslyn, E. V. *Coord. Chem. Rev.* **2003**, *240*, 3–15. (f) Martínez-Máñez, R.; Sancenón, F. *Coord. Chem. Rev.* **2006**, *250*, 3081–3093.

(2) (a) Mohr, G. J. *Chem.—Eur. J.* **2004**, *10*, 1082–1090. (b) Sessler, J. L.; Cho, D.-G. *Chem. Soc. Rev.* **2009**, *38*, 1647–1662.

(3) (a) Kim, T.-H.; Swager, T. M. *Angew. Chem. Int. Ed* **2003**, *42*, 4803–4806. (b) Zhang, S.-W.; Swager, T. M. *J. Am. Chem. Soc.* **2003**, *125*, 3420–3421. (c) Nolan, E. M.; Lippard, S. J. *Chem. Rev.* **2008**, *108*, 3443–3480.

(4) (a) Sun, S.-S.; Lees, A. J. *Chem. Commun.* **2000**, 1687–1688. (b) Miyaji, H.; Sessler, J. L. *Angew. Chem., Int. Ed.* **2001**, *40*, 154–157. (c) Anzenbacher, P., Jr.; Tyson, D. S.; Jursiková, K.; Castellano, F. N. *J. Am. Chem. Soc.* **2002**, *124*, 6232–6233. (d) Badugu, R.; Lakowicz, J. R.; Geddes, C. D. *J. Am. Chem. Soc.* **2005**, *127*, 3635–3641. (e) Palomares, E.; Martínez-Díaz, M. V.; Torres, T.; Coronado, E. *Adv. Funct. Mater.* **2006**, *16*, 1166–1170. (f) Jo, J.; Lee, D. *J. Am. Chem. Soc.* **2009**, *131*, 16283–16291. (g) Shang, L.; Jin, L.; Dong, S. *Chem. Commun.* **2009**, 3077–3079. (h) Gimeno, N.; Li, X.; Durrant, J. R.; Vilar, R. *Chem.—Eur. J.* **2008**, *14*, 3006–3012.

10.1021/ol1008558
Published on Web 05/10/2010

Scheme 1. CN^- Sensing by Nucleophilic or New SET-Based Reaction and Its STPs

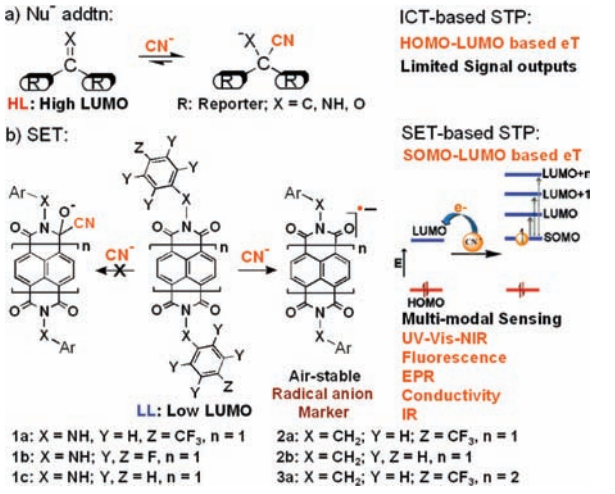

These indicators harness high-lying LUMO (HL), and thus, nucleophilic addition is preferred. They utilize internal charge-transfer (ICT)-based signal transduction pathway (STP) involving HOMO−LUMO-based electronic transition (eT). As a result, signal readability relies on a particular analytical technique, and instrumentation errors due to limited signal outputs become inevitable (Scheme 1a). In addition, some of them require elevated reaction temperature, biphasic conditions, and lag-time in sensing. This necessitates search for new indicators having new STPs which can circumvent the above problems.

In this context, single-electron transfer (SET) based biological sensors, e.g., redox-active cofactors in bacteria, $1e^-$ oxidation of cyanide, and its complex formation with cytochrome *c* oxidase (CcO), etc.,[7] motivated us to design molecules with new STP for anions which are anticipated to have easy and multiple signal readability.

As a proof-of-concept, herein we report the first SET-based cyanide indicator which is based on a low-LUMO (LL) design. We chose naphthalenediimide (NDI)[8a] and perylene-diimide (PDI)[8b] moiety as the core unit since (a) the NDI/PDI moieties have LL levels and provide synthetic scope to further lower them and (b) they contain carbonyl groups ideal for electron acceptance. This design aspect is crucial since for a given anion the electron-transfer component would be significantly larger in substrates having LL than for substrates having HL (Scheme 1b).[9]

This reaction-based system produces an air-stable radical anion marker, which is selective and sensitive (0.2−16 μM) to cyanide. This STP is based on a SOMO−LUMO based eT, a complete shift from the conventional HOMO−LUMO eT (Scheme 1b). The formation of spin and charge in the marker leads to multiple modes of sensing. The indicator exhibits regenerability and dip-stick sensing. Importantly, the high conductivity of the radical anion let us fabricate an electronic device for sensing cyanide.

We synthesized molecular indicators belonging to three classes: naphthalene-bis-hydrazimide (NBHI)[10] (**1a**−**c**), NDI (**2a**,**b**), and PDI derivatives (**3a**) with varying functionalities **X**, **Y**, **Z** and extent of core conjugation, *n*, and characterized by NMR, IR, and mass spectrometry.

Next, to confirm that the **Y**/**Z** groups and the linker **X** can indeed affect electron-withdrawing (EW) ability of the carbonyl groups and lower the LUMO levels, we carried out theoretical calculations and verified the results with IR and cyclic voltammetry (CV) (Supporting Information, Page No. S8 and S9). Figure 1 clearly depicts substantial lowering of

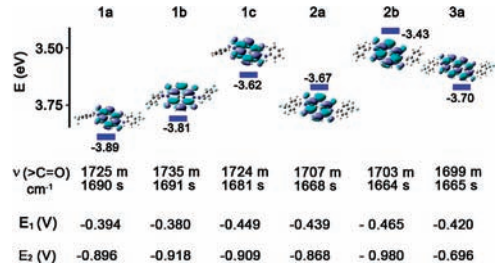

Figure 1. LUMO levels, IR frequencies, and reduction potentials for indicators **1a**−**3a**.

the LUMO levels going from **1c** → **1a** or **2b** → **2a** (effect of **Y**/**Z** groups) and also nicely discern the pivotal role of the linker **X** (NH/CH_2) in controlling the electron acceptor properties in NBHI (**1a**−**c**) versus NDI/PDI (**2a**,**b**, **3**).

The first electron reduction potential (E_1) also shows a significant lowering with substitution of the **Y**, **Z** and by the NH group. IR studies further substantiated that the EW ability of the carbonyl groups can be enhanced by substitution effects, e.g., stretching frequency of carbonyl groups in **1a** increases by 18 and 22 cm^{-1} compared to **2a**.

We then explored the colorimetric sensing ability of **1a** and **3a** in the presence of anions **1**−**14**. Only in the presence of cyanide do **1a** and **3a** with an extended core show an instantaneous change from colorless to dark brown and from an initial orange to a turquoise-blue solution, respectively (Figure 2). The other anions remained nonresponsive. These color changes are specific to the $1e^-$ transfer to the NDI/

(5) (a) García, F.; García, J. M.; García-Acosta, B.; Martínez-Máñez, R.; Sancenón, F.; Soto, J. *Chem. Commun.* **2005**, 2790–2792. (b) Tomasulo, M.; Sortino, S.; White, A. J. P.; Raymo, F. M. *J. Org. Chem.* **2006**, *71*, 744–753. (c) Chung, Y.; Lee, H.; Ahn, K. H. *J. Org. Chem.* **2006**, *71*, 9470–9474. (d) Yang, Y.-K.; Tae, J. *Org. Lett.* **2006**, *8*, 5721–5723. (e) Lee, K.-S.; Kim, H.-J.; Kim, G.-H.; Shin, I.; Hong, J.-I. *Org. Lett.* **2008**, *10*, 49–51. (f) Sessler, J. L.; Cho, D.-G. *Org. Lett.* **2008**, *10*, 73–75. (g) Cho, D.-G.; Kim, J. H.; Sessler, J. L. *J. Am. Chem. Soc.* **2008**, *130*, 12163–12167.

(6) (a) Hudnall, T. W.; Gabbbaï, F. P. *J. Am. Chem. Soc.* **2007**, *129*, 11978–11986. (b) Kim, Y.; Zhao, H.; Gabbaï, F. P. *Angew. Chem., Int. Ed.* **2009**, *48*, 4957–4960.

(7) Green, J.; Paget, M. S. *Nat. Rev. Microbiol.* **2004**, *2*, 954–966.

(8) (a) Bhosale, S. V.; Jani, C. H.; Langford, S. J. *Chem. Soc. Rev.* **2008**, *37*, 331–342. (b) Würthner, F. *Chem. Commun.* **2004**, 1564–1579.

(9) (a) Hoz, S. *J. Org. Chem.* **1982**, *47*, 3545–3547. (b) Hoz, S.; Speizman, D. *J. Org. Chem.* **1983**, *48*, 2904–2910.

(10) Compounds **1a** and **1b** were reported recently; see: Ajayakumar, M. R.; Mukhopadhyay, P. *Chem. Commun.* **2009**, 3702–3704.

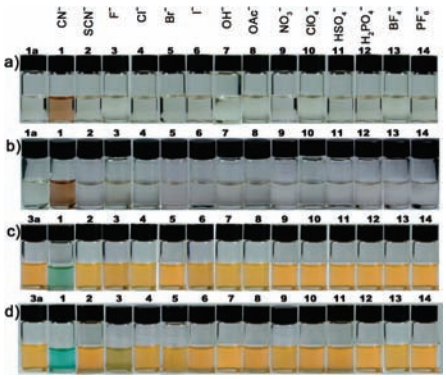

Figure 2. Photographs of **1a** in (a) DMF/H_2O (97:3); (b) DMF and **3a** in (c) THF/H_2O (97:3); (d) THF with anions **1**−**14**; [**1a**; 1.2×10^{-4} M, **1**−**14** in DMF/H_2O (97:3); 4.3×10^{-4} M and in DMF; 2.2×10^{-4} M, **3a**; 6×10^{-5} M, **1**−**14** in THF/H_2O (97:3); 9×10^{-4} M and in THF; 2.2×10^{-4} M].

PDI moiety[11] and indicates formation of the radical anion marker **1a**$^{\bullet-}$/**3a**$^{\bullet-}$. Importantly, the sensing could be performed under ambient conditions in mixed aqueous, polar aprotic, as well as nonpolar solvents. Because of the high air stability of the radical anion, no special precautions like glovebox were required during the sensing process.

The formation of the radical-anion marker during this sensing process would make it amenable to various spectroscopic techniques and provide diagnostic spectral signatures. Thus, to confirm our proposed SET-based reaction mechanism and to explore the multimodal signal readability, we verified the marker with UV−vis−NIR, fluorescence, EPR, IR, and electrochemical techniques.

UV−vis−NIR spectroscopy of **1a** show peaks at 358 and 377 nm. In the presence of cyanide, a new set of highly red-shifted peaks at 470, 603, 701, 786, and 1100 nm appeared (Figure 3a), while **3a** with cyanide shows a new set of peaks at

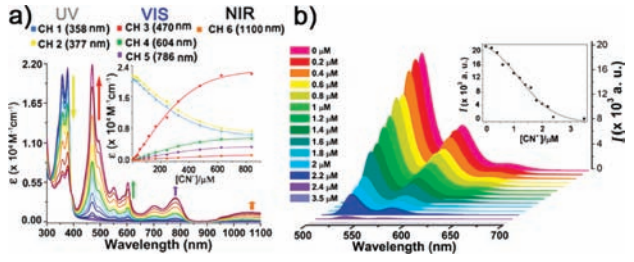

Figure 3. (a) UV−vis-NIR spectra showing the response of **1a** (1.2×10^{-4} M) upon incremental addition of CN^-, **1** in DMF. Inset shows the response of the optical channels as a function of CN^-. (b) Fluorescence spectra showing the response of **3a** (1.5×10^{-7} M) upon addition of CN^- in THF (excited at 485 nm). Inset show the plot of fluorescence intensity (*I*, integrated fluorescence from 500−700 nm) as a function of CN^-.

699, 761, 794, 952, and 1100 nm (Supporting Information, S10). These new peaks at 470−786 nm for **1a** and 699−952 nm for **3a** with cyanide and their relative intensity ratios perfectly match with the signature peaks due to $D_0 \rightarrow D_n$ eTs for the radical anions of the NDI and PDI moiety, respectively.[12] This validates formation of **1a**$^{\bullet-}$/**3a**$^{\bullet-}$ and also the SET-driven reaction.

The multioptical outputs for **1a**$^{\bullet-}$ (Inset of Figure 3) and the facile NIR absorption provides reliability in sensing cyanide and would also aid in reducing interference from biological chromophores.

We confirmed the air stability of the radical anion marker by UV−vis−NIR spectroscopy. The presence of clear isosbestic points and clean spectral plots for **1a**−**3a** in presence of cyanide point to an uncluttered SET process. Thus, **1a**$^{\bullet-}$ could be kept in open vials up to 3 h without decomposition, while in closed vials it could be stored at ambient temperature for a few weeks (Supporting Information, S11). Further, the radical anions of **1a**$^{\bullet-}$ upon oxygen purging were stable up to 35 min after which it shows slow decomposition. This confirms the high stability and applicability of this marker for sensing.

This stability of the radical anion originates from the number of low-energy charge delocalized resonating structures, which is dependent on the LUMO levels of the indicators (Supporting Information, S12). In order to experimentally confirm this, we compared the response of indicators **1a**−**2b** toward cyanide and hence its propensity to form the radical anion marker. Indeed, in line with the LUMO levels, the optical response and propensity to form the radical anion follows the order: **1a** > **1c** > **2a** > **2b** (Supporting Information, S12−S14).

We then explored the multiple signal outputs emanating from the radical anion as a consequence of cyanide sensing (Supporting Information, S15−S17). We chose **3a** due to its strong fluorescence. The SET-driven formation of **3a**$^{\bullet-}$ induces complete quenching of the 531−620 nm fluorescent bands within an extremely narrow concentration window of 0.2−3.5 μM of cyanide (Figure 3b).[13] The other strong evidence for the SET driven reaction comes from the diagnostic EPR signal unique to the imide radicals (g = 2.0056) of **1a**$^{\bullet-}$, formed in the presence of cyanide.[11] Square-wave voltammetry (SWV) also exhibited a cyanide specific 3-fold reduction in current and cathodic shifts of reduction waves of up to 20 mV. This is due to the fact that cyanide induced electron transfer makes it difficult to reduce **1a**. Similarly, the frequencies of carbonyl groups in **1a** at 1725 and 1690 cm^{-1} show a decrease in the intensity and new peaks arise at 1663 and 1625 cm^{-1} with cyanide as a result of greater degree of single bond character in the radical anion.

Compound **1a** was found to be highly selective toward cyanide in mixed-aqueous, polar aprotic, and nonpolar solvents; e.g., **1a** in DMF/H_2O (97:3) was found to be 2.1 $\times 10^2$, 1 $\times 10^2$, and 42 times more selective toward CN^-

(11) Andric, G.; Boas, J. F.; Bond, A. M.; Fallon, G. D.; Ghiggino, K. P.; Hogan, C. F.; Hutchison, J. A.; Lee, M. A.-P.; Langford, S. J.; Pilbrow, J. R.; Troup, G. J.; Woodward, C. P. *Aust. J. Chem.* **2004**, *57*, 1011–1019.

(12) Gosztola, D.; Niemczyk, M. P.; Svec, W.; Lukas, A. S.; Wasielewski, M. R. *J. Phys. Chem. A* **2000**, *104*, 6545–6551.

(13) Baggerman, J.; Jagesar, D.-C.; Vallée, R. A. L.; Hofkens, J.; De Schryver, F. C.; Schelhase, F.; Vögtle, F.; Brouwer, A. M. *Chem.—Eur. J.* **2007**, *13*, 1291–1299.

over F^-, $H_2PO_4^-$, and OH^-/OAc^-, respectively, while being completely nonresponsive toward other anions (Figure 4a).[14]

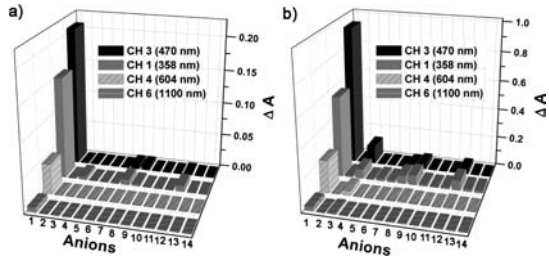

Figure 4. Selectivity profile of **1a** with anions **1**−**14** evaluated in terms of four optical channels: (a) DMF/H_2O (97:3) (**1a**, 1.2 × 10^{-4} M; **1**−**14**, 4.3 × 10^{-4} M) and (b) DMF (**1a**, 1.2 × 10^{-4} M; **1**−**14**, 2.2 × 10^{-4} M). ΔA refers to $A - A_0$, where A and A_0 stand for the absorbance in the presence and absence of anions, respectively.

When compared with other reducing anions, **1a** was ∼4 and 10 times more selective for cyanide over thiosulfate and dithionite, respectively, while ferrocyanide, nitrite, and sulfite remained completely nonresponsive (Supporting Information, S18 and S19). In DMF, **1a** was selective toward cyanide with respect to OH^-, OAc^-, $H_2PO_4^-$, and F^- by 38, 25, 22, and 8 times, respectively (Figure 4b). The other anions remained completely silent. No interference from reducing amine like hydrazine and from nucleophile/base like iodide and OH^- were observed. This specificity for cyanide was also confirmed with multiple signal outputs (Supporting Information, S20). The high specificity toward cyanide is supported by the well-known α-effect. The stability of radicals α to a lone pair is available only to cyanide in contrast to other anions studied here.[15]

Compound **1a** exhibited a highly attractive sensitivity toward cyanide in a diverse range of solvents. Sensitivity of 0.67 and 1.3 μM was achieved in THF and DMF. In DMF/H_2O (97:3), a sensitivity of 16 μM could be determined (Supporting Information, S20 and S21). An attractive sensitivity of 0.2 μM (∼ 5 ppb) in THF could be achieved by monitoring the fluorescence intensity of **3a**.

Since only a handful of sensors are known to sense cyanide on the solid surface,[4h] we analyzed the dip-stick sensing ability of **3a**. Interestingly, thin films of **3a** fabricated by vapor deposition technique onto glass substrates could detect cyanide in nonpolar solvents like petroleum-ether as well as in pure water (Figure 5a). Furthermore, the indicator systems show regenerability with an oxidizing agent like $NOBF_4$. The

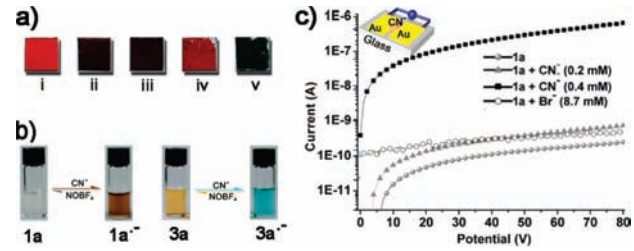

Figure 5. (a) Photograph depicting sensing of CN^-, **1** with thin films of **3a**: (i) 0 mM of **1**, (ii) 0.1 mM of **1** in petroleum ether, (iii) 0.2 mM of **1** in Pet. ether, (iv) 4 mM of **1** in water, (v) 8 mM of **1** in water. Photographs were taken after 90 min of soaking with **1** in water. (b) Regenerability experiments of **1a**/**3a** with CN^- and $NOBF_4$. (c) I−V curves of **1a** and with different amounts of **1** or **5**. Inset shows the two terminal electronic devices.

dark brown (**1a**$^{\bullet-}$) and the turquoise-blue (**3a**$^{\bullet-}$) solution formed in the presence of cyanide could be instantaneously switched to the original sensors **1a**/**3a** (Figure 5b).

Finally, we could successfully fabricate a cyanide sensing two-terminal device applying this SET-based reaction. The device consisted of two Au electrodes deposited on a glass plate with a gap of 80 μm (Figure 5c). Compound **1a** shows negligible current, however, with increasing amounts of cyanide; e.g., with 0.4 mM of cyanide, the current is more than 4 orders of magnitude higher than **1a**. No major increase in current was observed with excess of other anions (Supporting Information, S6).[16]

In conclusion, we have demonstrated a new SET-driven reaction which is highly selective and sensitive to cyanide. This new STP is completely different from the conventional HOMO−LUMO-based STPs known to date. The multiple signal outputs emanating from the radical anion marker and its spectroscopic signatures were duly characterized. The effect of the LUMO levels of the indicators on the cyanide response was evaluated. Air-stability and high conductivity of the marker allowed us to fabricate an electronic device for cyanide sensing.

Acknowledgment. We thank CSIR, DST and FIST-II for the financial support and Prof. P. K. Bharadwaj and Mr. R. K. Das (IIT Kanpur) for the EPR experiments. We thank the 500 MHz NMR facility at AIRF, JNU, and MALDI-TOF facility at CIF, SLS, JNU, New Delhi.

Supporting Information Available: Experimental procedures, synthesis, various spectroscopic data, and supplementary spectral data. This material is available free of charge via the Internet at http://pubs.acs.org.

OL1008558

(14) We were unable to use buffer solution for the DMF/H_2O experiment as the buffers interfered with the radical anion sensor.

(15) Edwards, J. O.; Pearson, R. G. *J. Am. Chem. Soc.* **1962**, *84*, 16–24. This extra stabilization of the radical has been explained on the basis of the MO diagram of a three-electron system, and this effect is predominant at carbonyl or other unsaturated carbons.

(16) Penneau, J.-F.; Stallman, B. J.; Kasai, P. H.; Miller, L. L. *Chem. Mater.* **1991**, *3*, 791–796.